CLEEN
Cluster for Energy and Environment

Research Report nr D337
Helsinki 2014

Jaakko Ylätalo, Tero Tynjälä

Report of CaL model development
Modelling CO_2 carrying capacity of lime particles over time

ccsp
Carbon Capture and Storage Program

CLEEN LTD
ETELÄRANTA 10
P.O. BOX 10
FI-00130 HELSINKI
FINLAND
www.cleen.fi

ISBN XXX-XX-XXXX-X
ISSN XXXX-XXXX

Cleen Ltd.
Research Report nr D337

Jaakko Ylätalo, Tero Tynjälä

CaL model development – Modelling CO2 carrying capacity of lime particles over time

ccsp
Carbon Capture and Storage Program

Cleen Ltd
Helsinki 2010

Report Title: CaL model development – Modelling CO_2 carrying capacity of lime particles over time

Key words: Calcium looping process, CO_2 carrying capacity, limestone, modelling

Abstract

This report describes the model development work done as part of the CCSP-project by LUT Energia as subcontracting to Foster Wheeler Energia Oy. The goal of this subcontracting package is to improve the reliability and modelling capabilities of the LUT calcium looping models. The development work concentrated on creating models to describe the CO2 carrying capacity of lime particles over time. The CO2 carrying capacity describes the ability of lime material to receive and release CO2 in the cyclic calcium looping process. The carrying capacity is dependent on the age fraction populations that exist in the system and develops a as function of several process parameters. Two different approaches were created that both can be implemented to the dynamic 1D calcium looping model framework. Earlier experimental work from different research groups on the aging of lime material was implemented to framework and continuum equations were written for the age fractions. Continuum equations were implemented to Excel and solved.

Lappeenranta, March 2014

Table of contents

1 Introduction

This report describes the model development work done as part of the CCSP-project by LUT Energia as subcontracting to Foster Wheeler Energia Oy. The goal of this subcontracting package is to improve the reliability and modelling capabilities of the LUT calcium looping models. The development work concentrated on creating models to describe the CO_2 carrying capacity of lime particles over time. The CO_2 carrying capacity describes the ability of lime material to receive and release CO_2 in the cyclic calcium looping process. The carrying capacity is dependent on the age fraction populations that exist in the system and develops a as function of several process parameters. Two different approaches were created that both can be implemented to the dynamic 1D calcium looping model framework. Earlier experimental work from different research groups on the aging of lime material was implemented to framework and continuum equations were written for the age fractions. Continuum equations were implemented to Excel and solved.

2 Calcium looping process

Post-combustion calcium looping was first introduced by Shimizu et al. (1999). This technique can capture CO_2 and SO_2 from static sources by utilizing a twin fluidized bed system. Flue gas from a stationary source is processed in a fluidized bed reactor, known as the carbonator. The carbonator captures CO_2 and SO_2 from the flue gas to solid calcium oxide at around 650 ºC. This forms calcium carbonate and calcium sulphate, $CaCO_3$ and $CaSO_4$, which are then transferred to a fluidized bed regenerator, known as the calciner. The calciner regenerates the carbonate back to calcium oxide at around 920-950 ºC. The regenerated calcium oxide is returned to the carbonator where it resumes capturing CO_2 from the flue gases. The formed calcium sulphate is stable in the loop and will accumulate to the system unless fresh calcium carbonate is fed to the system and the used sorbent is removed at a steady rate. The temperature difference between the reactors can be achieved by many means, burning suitable fuels in the calciner in an atmosphere of oxygen and recirculation gas or from external heat sources. This forms a highly concentrated CO_2 gas flow which can be compressed and transported to a storage site after steam and oxygen removal. As a result of solid fuel combustion, ash accumulates in the system which increases the need of solid purging from the loop. The general layout of the calcium loop is presented in Figure 1.

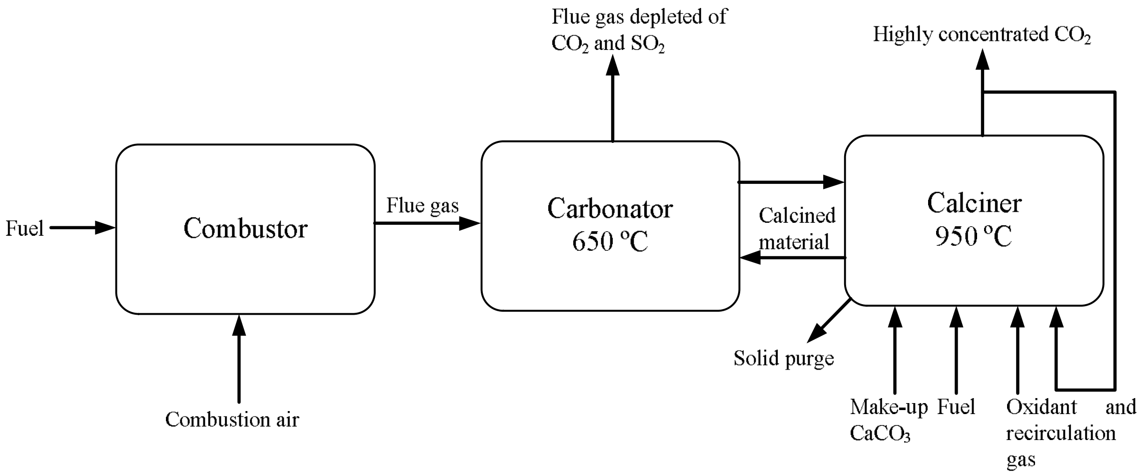

Figure 1. Concept of the calcium looping process.

3 Decrease of carrying capacity of lime in cyclic carbonation and calcination

One of the biggest challenges of the calcium looping process is the decrease of carrying capacity over carbonation and calcination cycles. That is why it is important to understand this phenomenon and model it accurately. Natural lime subjected to cyclic carbonation and calcination undergoes a radical change in physical and chemical properties. Extensive research has been done to understand the behaviour of lime in cyclic carbonation-calcination (Abanades, 2002; Abanades and Alvarez, 2003; Arias et al., 2011; Barker, 1973; Grasa et al., 2009; Stanmore and Gilot, 2005; Wang and Anthony, 2005).The general understanding is that during each high temperature calcination step the porous structure of the lime particle sinters weakening its ability to transfer CO_2 inside the particle. This causes the carbonation step to change from a fast kinetically controlled reaction to a diffusion controlled reaction, which in turn is not very suitable for post-combustion capture purposes. This phenomenon affects the performance of the calcium looping process significantly as shown in Figure 1. If one mole of calcium oxide can capture one mole of CO_2 in the first calcination–carbonation cycle, after 20 cycles 10 moles of calcium oxide is needed to capture that one mole of CO_2 in the residence times of a CFB reactor. Therefore, the looping ratio of lime between the reactors has to be 10 times the stoichiometric value or even higher if the unreactive components of the solid material are included. The particle porous structure will regenerate itself slowly if carbonation time is extended (Arias et al., 2011B). Correlations have been devised to predict the loss of activity in cyclic carbonation and calcination (Borgwardt, 1989; German and Munir, 1976; Wang and Anthony, 2005). The most commonly used approach in literature is the one formulated by Grasa and Abanades (2006) in which the maximum carrying capacity reaches a residual value asymptotically as a function of carbonation-calcination cycles

$$X_N = \frac{1}{\frac{1}{1-X_r} + fN} + X_r$$

where *f* represents the carrying capacity decay coefficient [-], *N* the number of full cycles and X_r the residual activity in molar fractions [-]. Grasa and Abanades (2006) suggested a value of 0.5 for the decay coefficient *f* and 0.075 for the residual activity. The correlation predicts quite well the maximum CO_2 carrying capacity of natural lime particles.

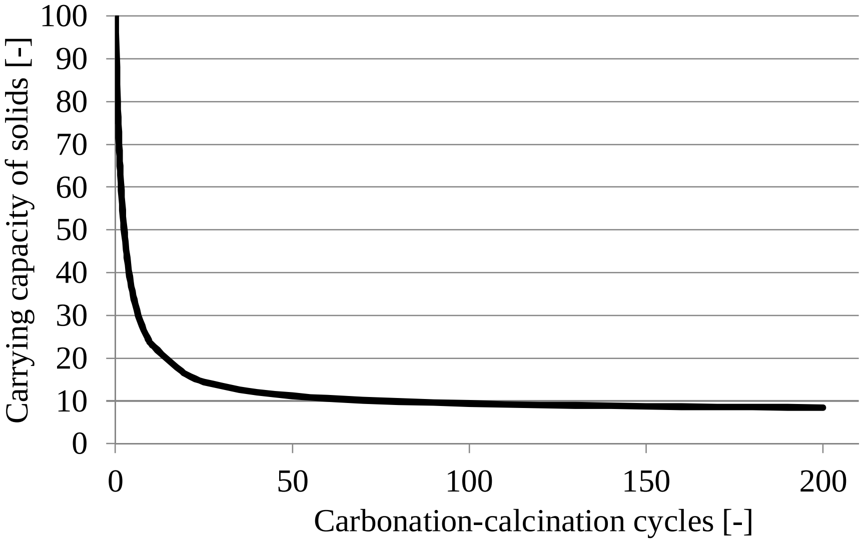

Figure 1. Carrying capacity of natural lime as a function of carbonation-calcination cycles plotted with the correlation of Grasa and Abanades (2006). A sharp decrease in CO_2 uptake can be noticed in the first ten cycles.

To compensate for this loss of activity, a make-up flow of fresh limestone has been introduced to the calciner reactor. This means that the solid material present in the system will have an age population with different reactive properties.

3.1 Modelling of the average carrying capacity: first approach

The actual carrying capacity of the system is defined by the age population of the system. The average carrying capacity can be calculated as a sum product of the different age fractions

$$X_{ave} = \sum_{N=0}^{N=\infty} X_N x_{Ca,N}$$

Where $x_{Ca,N}$ is the molar fraction of the age fraction N [-]. The transient carrying capacity can be tracked over time by tracking the development of age fractions in the system. This requires the formation of age fraction balances. Age fractions are global variables that are dependent on the behavior of both reactors. Figure 2 describes the mass/molar balance of the calcium looping system. The material ages over the cycle N [-] that is defined by the carbonate exchange between reactors, in other words, the cycle is the rate of aging for the material. Carbonate exchange between reactors is defined by the circulation ratio between reactors FR and the carbonator carbonate fraction in solids X_{carb} and calciner carbonate fraction in solids X_{calc}.

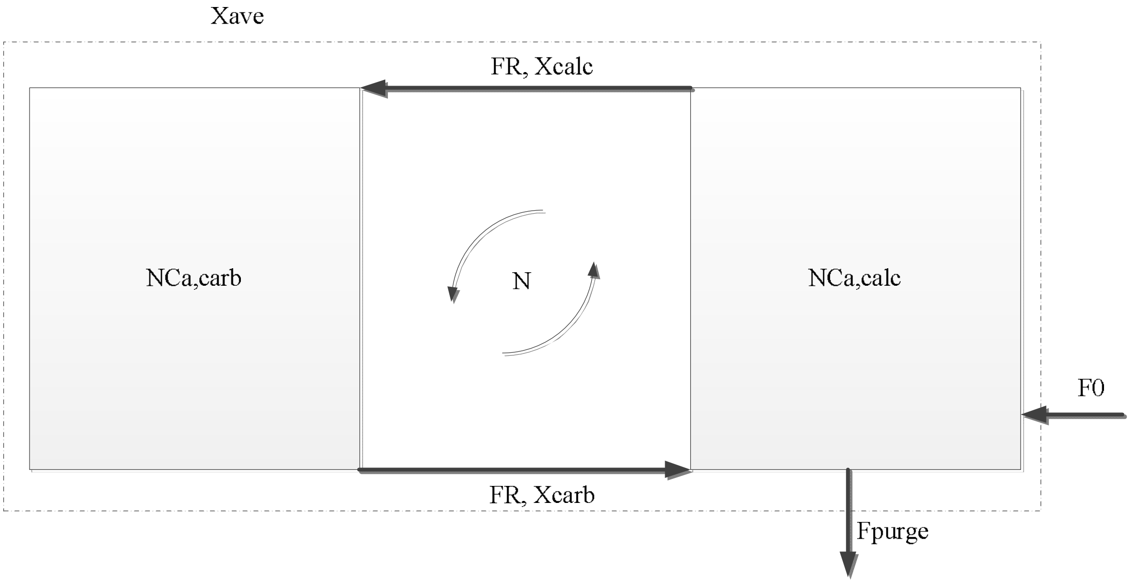

Figure 2. Age fraction mass/molar balance of calcium looping process.

Higher circulation rate and carbonate content in the solids from the carbonator means faster aging rate. Poor calciner operation and high carbonate content in the calciner solids means slower aging rate. Also the mass of calcium $N_{Ca,carb}$ + $N_{Ca,calc}$ in the system affects the transient behavior of the average carrying capacity. Make-up flow of limestone F_0 increases the fraction fresh lime (N=0) in the balance and purge F_{purge} removes evenly from all the fractions. With this basis, time derivatives for the age fractions can be formed

N=0

$$\frac{dx_{Ca,0}}{dt}=\frac{1}{N_{Ca}}\left(-F_R x_{Ca,0}\left(X_{carb}-X_{calc}\right)+F_0-x_{Ca,0}F_{purge}-x_{Ca,0}\frac{dN_{Ca}}{dt}\right)$$

N=1-∞

$$\frac{dx_{Ca,N}}{dt}=\frac{1}{N_{Ca}}\left(F_R x_{Ca,N-1}\left(X_{carb}-X_{calc}\right)-F_R x_{Ca,N}\left(X_{carb}-X_{calc}\right)-x_{Ca,N}F_{purge}-x_{Ca,N}\frac{dN_{Ca}}{dt}\right)$$

N=∞

$$\frac{dx_{Ca,\infty}}{dt}=\frac{1}{N_{Ca}}\left(F_R x_{Ca,\infty-1}\left(X_{carb}-X_{calc}\right)-x_{Ca,\infty}F_{purge}-x_{Ca,\infty}\frac{dN_{Ca}}{dt}\right)$$

Table 1. Parameters of the first calculation case adapted from Arias et al. 2005.

Parameters	Value	Unit
k	0.5	
Xr	0.075	
Δt	1	s
mCatot0	100	kg
nCa	1.8	kmol
qmCO2	0.1	kg/s
FCO2	0.002273	kmol/s
FR/FCO2	20	-
FR	0.045455	kmol/s
F0/FCO2	0.1	-
F0	0.000227	kmol/s
FCARB	0.002045	kmol/s
Xcarb	0.045	-
Xcalc	0	-
qn,purge	0.000227	kmol/s

The balance equations were implemented into Excel and age fractions were discretized based on cycles. Balances of Cycles from 0 to 200+ were solved time dependently where 200+ represents all cycles beyond 200 and the carrying capacity of that age fraction is the residual activity 0.075. Time derivatives of age fractions were calculated based on the time derivatives and selected time step.

$$x_{Ca,N}^{t+\Delta t} = x_{Ca,N}^{t} + \frac{dx_{Ca,N}}{dt}\Delta t$$

Where *Δt* is the time-step [s]. A calculation case was devised based on parameters acquired from the study of Arias et al. 2005. Parameters of the case are listed in Table 1. The circulation rate and make-up flow have been defined relatively to the carbon dioxide flow. Carbonate content exiting the carbonator is calculated based on the circulation ratio, average carrying capacity and CO_2 molar flow

$$X_{carb} = \begin{cases} X_{ave}, if \ \dfrac{E_{CO2}F_{CO2}}{F_R} > X_{ave} \\ else \ \dfrac{E_{CO2}F_{CO2}}{F_R} \end{cases}$$

where E_{CO2} represents the theoretical capture efficiency of the carbonator which is defined by the operation of the carbonator e.g. reactivity of lime, average temperature and residence time of solids. X_{calc} is dependent on the operation of the calciner but is assumed to be 0. Purge is selected to match the make-up molar flow but in reality it is determined by the total mass balance of the system.

Figure 3 presents average carrying capacity of the system plotted over time. The solid mass considered to be fresh material (N=0) when initializing the simulation. The average carrying capacity decreases slowly to the steady-state value that is around 0.42 defined by the make-up flow over a period of two hours.

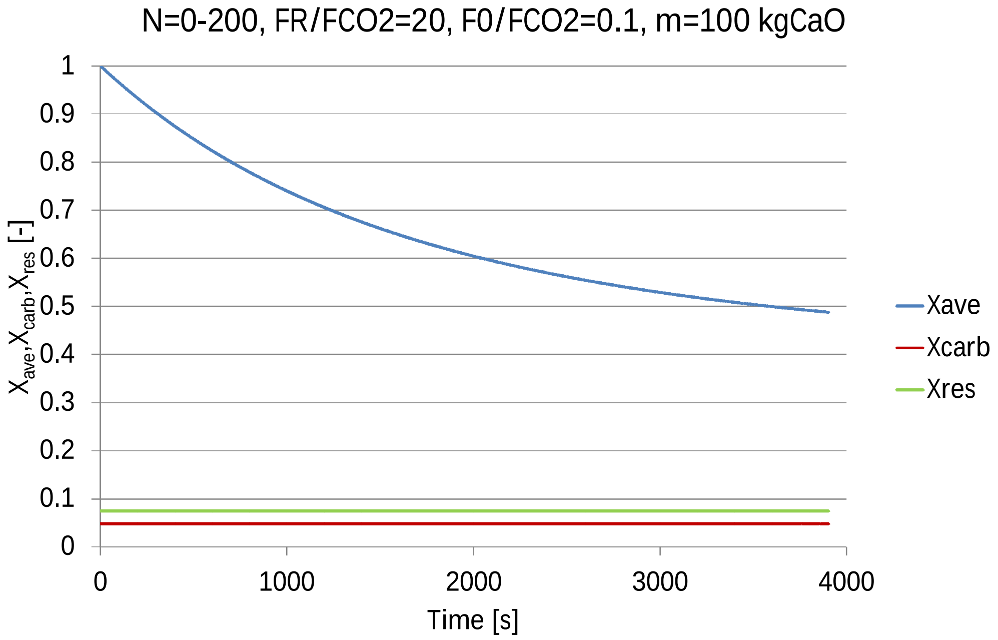

Figure 3. Time dependent average carrying capacity of the lime. Carbonation conversion and residual activity plotted also as function of time.

In conclusion, this approach is time accurate and can be used to track single age fractions. The downside of this approach is the use of resources to solve one time dependent variable, average carrying capacity. The calculation matrix for this case is 200 * 7200 for a two hour period of simulation time. By discretizing the age fractions differently, the size of the matrix could be reduced. The simplest matrix in this approach can be made using three age fractions but accuracy of the estimate would suffer Figure 4.

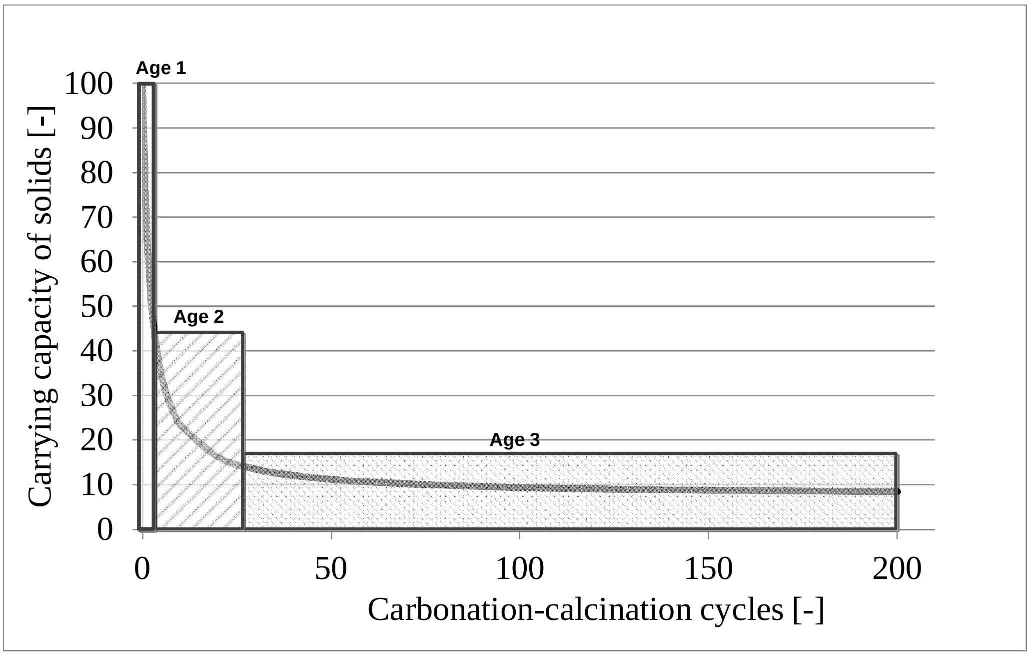

Figure 4. Discretization of carrying capacity to three age fractions.

3.2 Modelling of the average carrying capacity: second approach

Another, simpler approach could be achieved by calculating the steady-state carrying capacity based on operational parameters and using the system time constant to account for transient changes. The steady-state average carrying capacity can be solved using the approach proposed by Abanades et al. (2002) applying an analytical solution to geometrical progression. Here Xr is 0.174 and f 0.782 because of the different function form used in the research paper for the value of carrying capacity X_N.

$$X_{ave} = \frac{fF_0}{F_0 + F_R(1-f)} + X_r$$

The time dependent carrying capacity can be defined the same way as the age fractions

$$X_{ave}^{t+\Delta t} = X_{ave}^{t} + \frac{dX_{ave}}{dt}\Delta t$$

Derivative of the average carrying capacity is defined by the system time constant and the difference between two states. In this case the make-up flow is F_0 changing over time.

$$\frac{dX_{ave}}{dt} = \frac{X_{ave}(F_{0,t1}) - X_{ave}(F_{0,t2})}{\tau}$$

The time constant of the system is defined by the total moles of Ca in the system and the carbonate exchange rate between reactors and the make-up

$$\tau = \frac{N_{Ca}}{F_R\left(X_{carb} - X_{calc}\right) - F_0}$$

This method does not allow the physical modelling of different age fractions or the delay of age in the bed material, only the calculation of the change between different carrying capacity states. The benefit of this method is low computational strain, simplicity and numerical stability. Figure 5 presents the evaluation of carrying capacity in steady-state with the same process parameters as in the previous case and the dynamic change in average carrying capacity when make-up flow is reduced. Steady-state average carrying capacity is 0.42 as in the previous case. The step change in make-up flow decreases carrying capacity to 0.21.

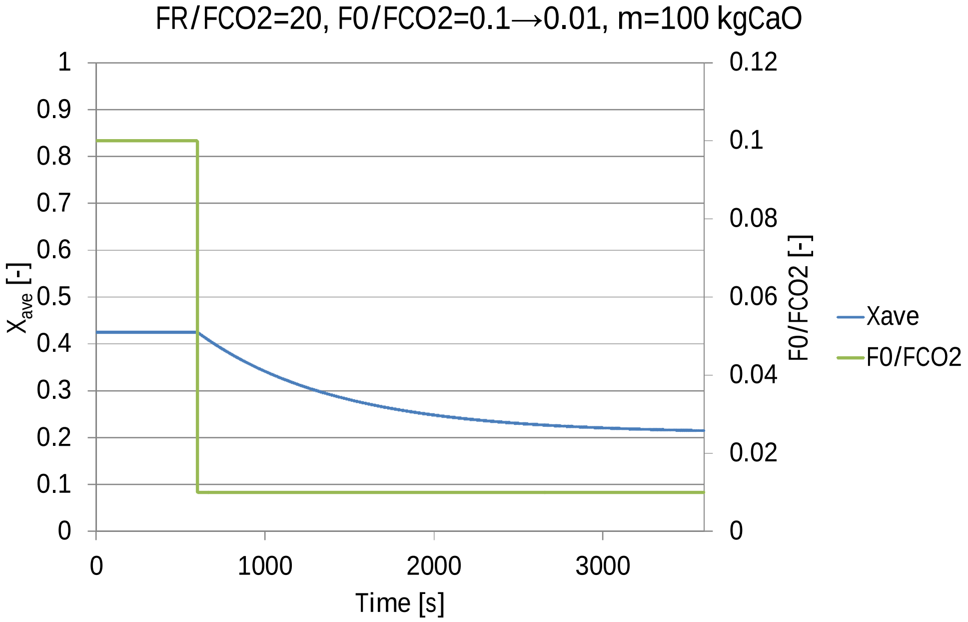

Figure 5. Evaluation of the average carrying capacity with the state-to-state method. Step like changes in the make-up cause a slow decrease in the average carrying capacity.

In conclusion, two methods were created to evaluate the average carrying capacity in the calcium looping system. Both models can be incorporated to the calcium dynamic 1D calcium looping model framework. The simpler model is more suitable to steady-state analysis with less computational strain. The more complex model that calculates age fractions can be used to model the phenomenon with increased accuracy including transient behavior in the material.

References

Abanades, J.C. (2002). The maximum capture efficiency of CO2 using carbonation/calcination cycle of CaO/CaCO3. *Chemical Engineering Journal*, 90, pp. 303-306.

Abanades, J.C. and Alvarez, D. (2003). Conversion limits in the reaction of CO2 with lime. *Energy & Fuels*, 17, pp. 308-315.

Arias, B., Abanades, J.C., and Grasa, G. (2011). An analysis of the effect of carbonation conditions on CaO deactivation curves. *Chemical Engineering Journal*, 167, pp. 255-261.

Arias, B., Abanades, J.C., and Anthony, J.C. (2011B). Model for self-reactivation of highly sintered CaO particles during CO2 capture looping cycles. *Energy & Fuels*, 25, pp. 1926-1930.

Barker, R. (1973). Reversibility of the reaction CaCO3 = CaO + CO2. *J. Appl. Chem. Biotechnol.*, 23, pp. 733-742.

Borgwardt, R. (1989). Sintering of nascent calcium oxide. *Chemical Engineering Science*, 44, pp. 53-60.

German, R. and Munir, Z. (1976). Surface area reduction during isothermal sintering. *Journal of American Ceramic Society*, 59, pp. 379-383.

Grasa, G. and Abanades, J.C. (2006). CO2 capture capacity of CaO in long series of carbonation calcination cycles. *Industrial & Engineering Chemistry Research*, 45, pp. 8846-8851.

Grasa, G., Murillo, R., Alonso, M., and Abanades, J.C. (2009). Application of the the random pore model to the carbonation cyclic reaction. *AIChE Journal*, 55, pp. 1246-1255.

Shimizu, T., Hirama, T., Hosoda, H., Kitano, K., Inagaki, M., and Tejima, K. (1999). A twin fluid-bed reactor for removal of CO2 from combustion processes. *Trans IChemE*, 77, pp. 62-68.

Stanmore, B. and Gilot, P. (2005). Review - calcination and carbonation of limestone during thermal cycling for CO2 sequestration. *Fuel Processing Technology*, 86, pp. 1707-1743.

Wang, J. and Anthony, E. (2005). On the decay behaviour of the CO2 absoprtion capacity of CaO-based sorbents. *Insdustrial & Engineering Chemistry Research*, pp. 627-629.